ORIGINAL ARTICLE

Influence of graphene-enriched nanofluids and textured tool on machining behavior of Ti-6Al-4V alloy

Rupinder Singh[1] · J. S. Dureja[2] · Manu Dogra[3] · Munish Kumar Gupta[4] · Mozammel Mia[5]

Abstract

In this study, turning of titanium (Ti-6Al-4V) alloy under four different environments as dry, vegetable oil under minimum quantity lubrication (MQL), texture on the rake face filled with graphene particles, and graphene-mixed vegetable oil under nanoparticle-based minimum quantity lubrication (NMQL) with textured carbide tools is investigated. Results shows that maximum tool life, lower cutting forces, and minimum cutting temperature generated are with NMQL followed by MQL, texture filled with graphene, and dry turning. The tool life under NMQL is improved by 178 to 190%, main cutting force minimized by 36 to 40%, and cutting temperature reduced by 31 to 42% as compared with dry condition at various cutting speeds. The best turning performance is achieved under NMQL which is mainly due to higher thermal conductivity of MQL fluid mixture and shearing action imparted by graphene on different contact surfaces of tool. Further, the phenomena of improved thermal conductivity and shearing action imparted by graphene are explained by using transient hot-wire/SEM/Raman spectroscopy in this study. Finally, it is concluded that graphene has potential to act as lubricant/coolant in turning processes.

✉ Munish Kumar Gupta
munishgupta@sdu.edu.cn

Rupinder Singh
rupinder_singh302@yahoo.com

J. S. Dureja
jsdureja73@gmail.com

Manu Dogra
mdogra7@gmail.com

Mozammel Mia
mozammelmiaipe@gmail.com

[1] Department of Mechanical Engineering, University School of Engineering & Technology, Rayat Bahra University, Mohali, Punjab, India

[2] Department of Mechanical Engineering, Punjabi University, Patiala, Punjab, India

[3] Department of Mechanical Engineering, Panjab University SSG Regional Centre, Hoshiarpur, Punjab, India

[4] Key Laboratory of High Efficiency and Clean Mechanical Manufacture, Ministry of Education, School of Mechanical Engineering, Shandong University, Jinan, Shandong, People's Republic of China

[5] Department of Mechanical and Production Engineering, Ahsanullah University of Science and Technology, Dhaka 1208, Bangladesh

Nomenclature

MQL	Minimum quantity lubrication
NMQL	Nanoparticle-based minimum quantity lubrication
F_x	Axial thrust force (N)
F_y	Radial thrust force (N)
F_z	Main cutting force (N)
VB_{max}	Maximum flank wear (μm)
V_c	Cutting speed (m/min)
f	Feed (mm/rev)
a_p	Depth of cut (mm)
r_e	Nose radius (mm)
HRC	Rockwell hardness on C scale
SEM	Scanning electron microscope
ASTM	American Society for Testing and Materials
ISO	International Organization for Standardization
L/D	Length to diameter ratio
T1	Dry textured tool
T2	Textured tool with canola oil as MQL based
T3	Textured tool filled with graphene
T4	Textured tool with graphene mixed in canola oil as NMQL fluid

1 Introduction

In turning, the force exerted by single point cutting tool for deformation of the workpiece material is transformed into heat [1]. The greater part of this heat is taken away by chips, partly goes to the specimen, and some carried away by a cutting tool. The heat, which goes to workpiece and tool, results in deterioration of both machined workpiece surface quality and tool life [2]. For reducing the negative effect of heat during turning, conventional cutting fluids (mineral oil, aqueous-based oil, synthetic, and semi-synthetic) are being used for cooling/lubrication purpose [3]. However, use of these fluids leads to economic, ecological, and health-related issues and also increase the production cost. This has motivated the researchers to switch over to environmental friendly and sustainable alternatives for improved machining performance as compared with conventional cutting fluids [4].

In the past, the concept of dry machining has attracted the affection of research community [5, 6]. However, there are troubles related with heat dissipation, surface integrity, and wear on tool throughout machining of difficult-to-cut materials under dry conditions [7]. Therefore, to overcome above-mentioned negative results of dry turning, other sustainable alternatives are required particularly for machining of hard-to-cut materials.

For enhancing the performance of turning operation and to decrease the use of conventional cutting fluids, MQL technique has been explored by the investigators in the recent past [8]. In MQL generally (10–100 ml/h), quantity of cutting fluid is required, thus this is a sustainable alternative to conventional flood machining [9]. MQL can lower the overall machining cost and expenditure associated with the disposal of cutting fluid. To further enhance the sustainability, various types of vegetable fluids (soybean based, sunflower, coconut oil, canola oil, groundnut oil, shear butter oil, olive oil) and nano solid lubricants have been explored under MQL [10, 11]. Vegetable oils are biodegradable, non-toxic, having good lubricity, provide high strength lubricating film, have a higher flash point, higher viscosity index, and better boiling point [12]. Similarly, the solid lubricants are eco-friendly, biodegradable, and less toxic in nature. In the past, researchers have tried different types of nanoparticles/additives as lubricants (graphite, titanium dibromide (TiB$_2$), calcium fluoride (CaF$_2$), molybdenum disulfide (MoS$_2$), cerium fluoride, boric acid (H$_3$BO$_3$) boron nitride, talc, tungsten disulfides

(WS$_2$), aluminum oxide (Al$_2$O$_3$), silicon dioxide (SiO$_2$), carbon nano-tubes (CNTs), and silicon carbide (SiC) [13, 14] copper oxide (CuO), phosphate ester, and hydrocarbon compound [2], under machining. Su et al. [15] in their work found that graphite mixed nanofluid under MQL, minimizing the cutting forces by 26% and cutting temperature by 21% as compared with dry turning. Rapeti et al. [13] mixed particles of nano MoS$_2$ with different vegetable oils under MQL environment. Results indicated that use of nanoparticles-based MQL fluid lead to reduced tool wear, cutting force, cutting temperatures, and surface roughness in contrast to all other selected environments. Yi et al. [16] compared performance of ROCOL_Ultracut clear (CC coolant) with graphene oxide (GO) nanofluids and investigated that due to improved dispersion of GO nanofluid under higher pressure lowers down the cutting temperature by 4.04% w.r.t. CC coolant used. Further, higher feed rate raised the cutting load, which in turn enhanced the elastic/plastic deformation which resulted in increase in temperature, but this trend was lower with GO in contrast to CC coolant. Likewise, Maruda et al. [2] found that the addition of phosphate ester–based anti wear additive resulted in lower friction at the contact zone, which in turn reduced the selected surface topography parameters by 6–38% as well as flank wear by 23% in contrast to dry machining. This was mainly due to highly concentrated anti wear phosphorus tribofilm on the machined surface. In another study [17], the consequence of MQL cooling and dry turning on the structural/micro-hardness transition of AISI 1045 steel has been studied. It was observed that MQL cooling resulted in a 40% reduction in depth of hardened layer along with 50% drop in surface crinkle zone after restricting the plastic deformations as compared with dry environment. Further, keeping in mind about the chief purpose of MQL, i.e., correct supply of cutting fluid, diameter of the falling mist drops at the cutting zone, nozzle distance from the cutting zone extensively studied [18]. The obtained results showed that the nozzle at a distance of 0.4 m from the contact zone enhanced the wettability of mating surface as well as provide optimum diameter of mist droplets.

Recently, researchers have also explored surface structuring of turning tools to enhance tribological performance [19–23]. For generating textures photolithography, electric discharge machining, and laser surface texturing techniques were used by the researchers [19]. Surface texturing on tool rake face produced less friction, lowers tool-chip contact area, and lowers chip-curl diameter in turning. Additionally, during turning, texture patterns

Table 1 MQL turning test conditions

Symbol/type of lubrication	Condition
T1/dry	Dry textured tool
T2/MQL	Textured tool with canola oil
T3/Self-lubrication	Textured tool filled with graphene on the rake face
T4/NMQL (Nanoparticle-based minimum quantity lubrication)	Textured tool along with graphene (1.0 wt%) mixed in canola oil

Table 2 Composition of alloying element in Ti–6Al–4V alloy [wt%]

| Al	C	Fe	N	V	H	O	Ti
5.90	0.08	0.30	0.03	3.80	0.01	0.14	Balanced

by trapping lubricant within their recesses ensured the continual supply of fluid to further improve the tool life [20, 21]. To develop texture patterns, different geometries like circular, grooves, oval have been used by the investigators in the past [19, 21]. The direction of the patterns as elliptical, parallel, linear, inclined, wavy, cross-patterned etc. were developed [16, 18–21]. But, some of the issues with laser surface texturing are as follows: the heat-affected zone, surface deformities (burrs or swells), and the formation of periodical surface structures. Frictional behavior is additionally influenced by swells, as they have significant height [19]. To overcome structuring deficiencies aspects, solid lubricants generally filled on rake face of the textured tool and thus forming a lubricating layer on tool-chip contact during turning [19, 21].

Researchers [21, 22] filled textures with MoS_2, and reported amelioration in cutting process regarding improved quality of machined surface along with tool life. Arulkirubakaran et al. [24] produced parallel, perpendicular, and cross-patterned textures on the rake surface of tool for turning of titanium (Ti-6Al-4V) alloy. MoS_2 mixed synthetic oil was used as cutting fluid during turning. The cutting force (10–20%) and temperature (17–23%) were reduced with perpendicular textured tool in

comparison with untextured tool. Contrary to this, Li et al. [25] reported that cutting forces were reduced by 3–11% and friction coefficient lowered by 8% with parallel textured tool during dry turning of Ti-6Al-4V alloy as compared with perpendicular textured tool. Ge et al. [20] found that surface textures with 50-μm groove width improved the infiltration of the cutting oil, which further enhanced the lubrication/cooling effect at the tool-chip mating surface, and considerably lessened the main cutting force (F_z) and tool wear by 24–63%, 63–83% in contrast to untextured tool. Hao et al. [26] developed amphiphobic nano-/micro-, micro-textures by pulsed fiber laser. The results revealed that nano-/micro-textured tool has less wettability angle (for water 135°)/(for oil 145°) which further helped in reduction of cutting force (6.25%), friction coefficient (9.73%), and the cutting temperature (9.01%) while compared with untextured tool under MQL turning.

Kiyota et al. [27] and Obikawa et al. [28] described that circular textures parallel to the tool cutting edge were more productive than perpendicular textures.

The use of carbon-based solid lubricant with textured tool under eco-friendly MQL has not been explored yet in turning. Literature shows that a complete study covering optimization of critical texturing parameters along with performance evaluation of textured tools under different cooling/lubrication environment for sustainability is not available. In particular, the study on turning of Ti-6Al-4V alloy with textured tools under the influence of graphene based MQL is not yet carried out. In the view of the above discussion, optimization of

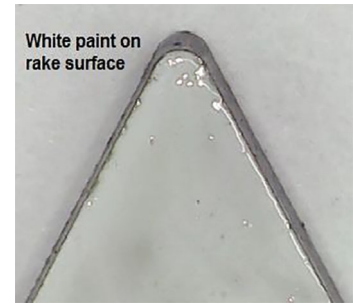**Fig. 1** Tool design and characterization
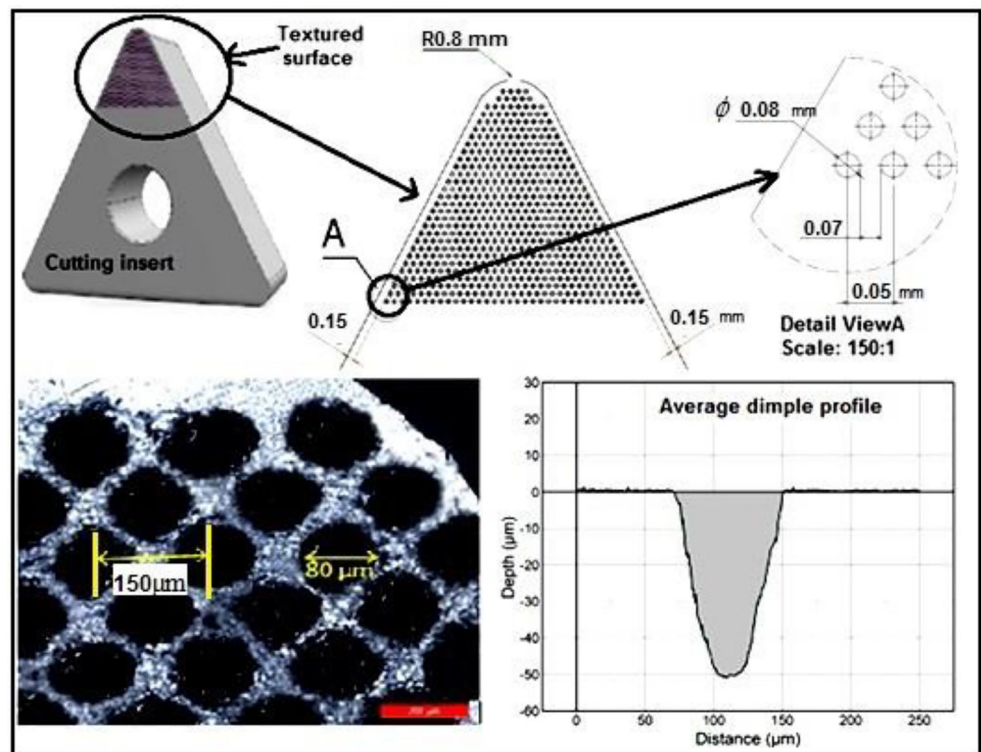
Table 3 Reduction in area of contact of chip on tool rake surface
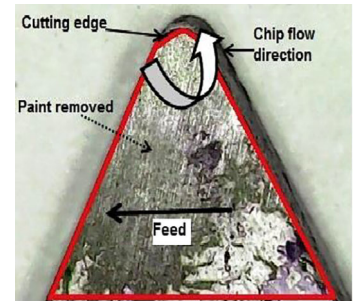
White paint on rake surface of tool	
Area up to paint removed	6.90 mm^2
Area of total textured surface having dimples up to removed paint surface	2.9 mm^2
Reduction in area up to removed paint surface after textures	4 mm^2

critical texture parameters was performed under various environments as indicated in Table 1. The performance of turning was assessed in terms of cutting forces, flank wear (VB$_{max}$), and cutting temperature.

2 Materials and methods

2.1 Work material

The specimen specified for experiments was commercially procured Ti-6Al-4V aerospace alloy. This material offers high strength and depth hardenability (32 HRC). The material is widely used in important aerospace components like fuselage, hydraulic tubing, bulk head, wing spar, landing gear, and jet engines applications [11, 16, 24]. The diameter and length of the workpiece were 32 mm and 100 mm, respectively, in order to maintain L/D ratio ≤ 10 as per (ISO 3685:1993) standard. The workpiece chemical composition is mentioned in Table 2.

2.2 Tool material and fabrication of texture

The turning insert having grade of TNMA160408THM (Make: WIDIA) with tool geometry (nose radius–r_e, 0.8 mm; rake angle, − 5°; clearance angle, 5°; inclination angle, 6°; major cutting edge angle, 90°) was chosen for
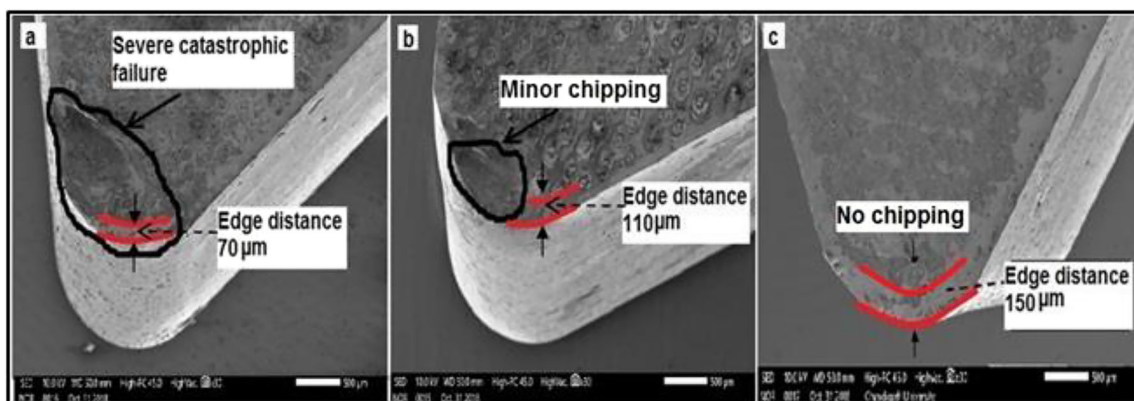
Fig. 2 Micrographs showing insert condition after 3.5 min of machining time

Table 4 Technical specifications of graphene

Graphene	Description
Color	Black powder
Purity	> 99%
Average thickness (z)	2–4 nm
Thermal conductivity	~ 3000–5000 W/mk
Average lateral dimension (X&Y)	10–15 μm
Number of layers	2–4 layers
Surface area	~ 350 m^2/g

experimentation. This was mainly selected because of no coating and chip breaker, which helps in easy fabrication of textures and further, to explore the participation of lubricant on the tool rake surface. In order to generate the texture on the tool rake surface, dimple patterns were selected as indicated in Fig. 1 [29]. The design process selected for texturing has been based on decreasing the area of contact of chips on the tool rake surface [21, 22]. Dimples were generated on the rake surface of the insert with femtosecond laser (with wavelength 1064 nm, pulse duration 10 ns) [21]. The diameters of dimples were 80 μm and 50 μm deep and the center distance between each dimple is 150 μm, as shown in Fig. 1. Optimizations of critical parameters related to texture were carried out as explained in Section 2.2.1. The newly developed textured inserts then cleansed through a 10-min ultrasonic-bath in acetone solution.

2.2.1 Optimization of texture parameters

First of all, preliminary experiment (V_c = 130 m/min, f = 0.10 rev/min, a_p = 0.2 mm) was executed for 2 min of machining time by painting white paint on rake face of the tool. This was carried out to observe the tool-chip contact area in order to estimate the texturing area on the tool rake face. As indicated in Table 3, sliding of chip covered 6.90 mm^2 area on the painted rake face of the cutting tool. Hence, we confine this study to produce textures on 6.90-mm^2 area near the cutting edge of the tool.

Further, it is significant to decide that at what distance from the cutting edge, texture fabrication should start—as texturing too near the cutting edge may weaker the cutting edge and tool can undergo catastrophic failure. Also, texturing too far from the edge may dilute the purpose of reducing the chip-tool contact surface area. In literature, work pertaining to optimization of edge distance is scant. But as per the cutting dynamics is concerned, this distance may affect the tool life significantly. Thus, in this study, it was decided to optimize the cutting edge distance. For which, another set of experimentation at (V_c = 130 m/min, f = 0.10 rev/min, a_p = 0.2 mm) with three cutting edge distances was conducted. Majority of researchers in the past have taken this edge distance as 100 μm [21, 28]. So, it was decided to select three edge distances as 70 μm, 110 μm, and 150 μm for preliminary experiments. On the basis of experimentation, it was observed that at 70-μm edge distance, severe catastrophic failure of tool occurred as shown in Fig. 2(a). For the 110-μm edge distance, there was minor chipping (Fig. 2(b)), whereas for 150-μm edge distance there was no chipping, which further indicated that for maintaining the edge strength, it is indispensable to take optimum distance from main cutting edge to start of texture, which was found to be 150 μm, as indicated in Fig. 2(c).
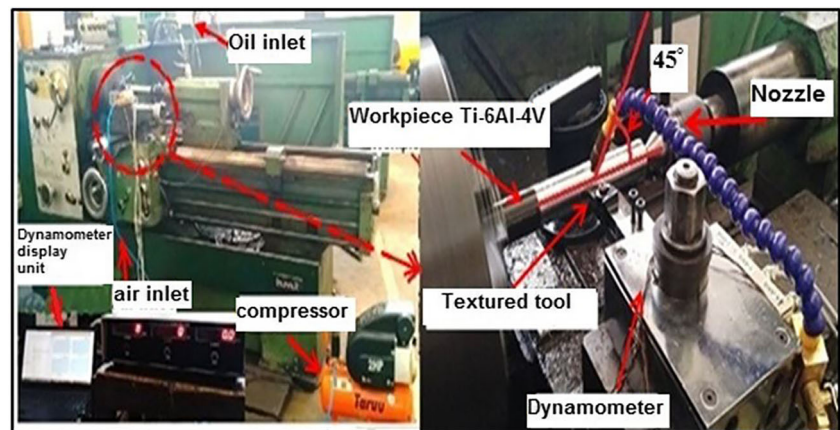
2.3 Graphene

Solid lubricant selected to be used in this study was commercially procured graphene. Solid lubricant such as MoS_2 will not work appropriately if O_2 and H_2O molecules are present during lubrication. Contrary to this, boric acid and graphite will not perform lubrication without moisture in the surrounding environment. Next, solid lubricants owing to their limited thickness ultimately wear out and lose their efficiency [30]. Consequently, due to layered structure, high thermal conductivity, environmentally insensitive, highly durable, chemically inert, easy shear capability graphene can perform as a prospective solid lubricant in various tribological applications [31, 32]. The technical specifications of used graphene are listed in Table 4 [33]. Due to high mechanical strength of graphene, it acts as a strong lubricant to lessen friction [34]. The function

Table 5 Thermal conductivity w.r.t. nanoparticle concentration at room temperature

| Sr. no	Type of fluid	Thermal conductivity W/mk
1	Canola oil	0.153
2	Graphene mixed in canola oil (0.2 wt%)	0.159
3	Graphene mixed in canola oil (0.5 wt%)	0.166
4	Graphene mixed in canola oil (1 wt%)	0.181
5	Graphene mixed in canola oil (2 wt%)	0.176

Fig. 3 Photographic view of the experimental setup

of graphene to act as effective lubricant has previously been confirmed by researchers in their experimental works [31–33]. Thus, from past works, it was chosen to investigate the tribological behavior of graphene in turning with the use of textured carbide tools.

2.4 Nanoparticle-based minimum quantity lubrication (NMQL)

In this work, canola vegetable oil was selected and mixed with graphene to be used under MQL. The value of thermal conductivity of canola oil is listed in Table 5. High viscosity of canola oil imparts more effective lubrication at the tool-chip contact surface, hence decreases the friction among the tool-chip/tool-workpiece contact area. The detail of nanoparticle-based minimum quantity lubrication (NMQL)-assisted experimental setup is shown in Fig. 3. The graphene loadings of 0.2, 0.5, 1.0, and 2.0% by weight were added to canola oil. Furthermore, to confirm heat carrying capacity of graphene blended with canola oil, the thermal conductivity tests utilizing a transient hot-wire (KD2 Pro system) were conducted at room temperature, as indicated in Table 5. The outcomes revealed that an addition of various wt% of graphene results in
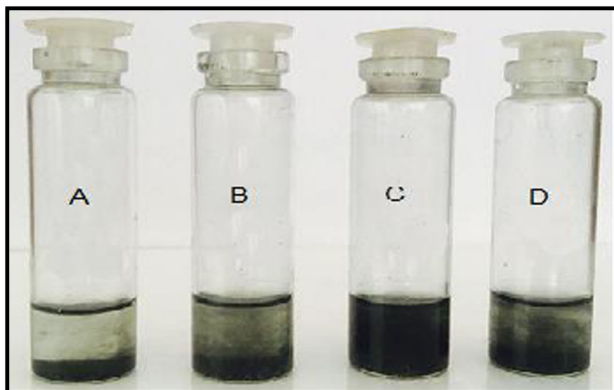
thermal conductivity enhancement by ~ 4.52, ~ 8.39, ~ 21.29, and ~ 14.19% of base oil.

Further, the suspension stability analysis was also carried out to ensure best suitable solution of graphene and canola oil w.r.t. added wt%. The aim was to attain a steady colloidal suspension of the different mixtures. After ultrasonication, different prepared mixtures were placed into glass flasks as shown in Fig. 4. The particles with 0.2, 0.5, and 2.0 wt% were separated only within a 24-h period. On the other hand, graphene-mixed oil (1 wt%) display particles stability up to 72 h.

2.4.1 Preliminary experiments to check performance of graphene mixtures into oil

Preliminary experiments for 3.5 min of machining time were conducted to test the performance of various prepared mixtures at varying V_c (80, 130, 180) m/min and fixed f (0.10 mm/rev.), as well as a_p (0.2 mm) as prescribed in Table 6. As this study was focused on finish turning and also as per the literature, cutting speed observed to be the most dominating factor, so for preliminary experimentation only cutting speed was varied. MQL parameters, i.e., (nozzle distance, 30 mm; air pressure, 6 bar; flow rate, 120 ml/h) were selected [5]. The nozzle direction with horizontal angle 45° and vertical angle 45° was chosen (Fig. 3) [35]. The results of preliminary experiments (Table 6) depicts that in contrast to different wt% of graphene, the least values of cutting force, flank wear, and cutting temperature were measured with 1 wt% of graphene-mixed solution. Therefore, on the basis of the above-mentioned all preliminary tests, the optimum value of graphene mixed in canola oil was found to be 1 wt%. Thus, for final experimentation, 1 wt% graphene was considered for mixing into canola oil.

2.5 Filling of texture

The lubricant was mixed with dispersing solvent isopropyl alcohol and then pressed into the dimples with the aid of a

Fig. 4 Suspension stability of graphene in canola oil (A: 0.2 wt%, B: 0.5 wt%, C: 1.0 wt%, D: 2.0 wt%) after mixing

Table 6 Performance of different mixtures obtained with different wt% under MQL

V_c (m/min)	wt%	Temperature (°C)	Main cutting force–F_z (N)	Flank wear (μm)
80	0.2	453	226	66
	0.5	442	220	51
	1.0	415	210	42
	2.0	462	232	91
130	0.2	610	221	82
	0.5	597	205	63
	1.0	582	198	55
	2.0	624	228	107
180	0.2	642	216	86
	0.5	630	202	75
	1.0	612	190	64
	2.0	646	223	116

dropper. Finally, the textured inserts filled with graphene were obtained after drying out the solvent [22]. The use of graphene in this study was new; so, it was decided to perform preliminary experiments to study the effects of V_c, f, and a_p on turning under the influence of graphene.

2.5.1 Preliminary experiments for finalizing the machining parameters

As indicated in Table 7, textured tools were tested for 3.5 min of machining time under NMQL. The results of preliminary study are presented in Table 8. From the results, it was deduced that at highest level of speed and feed used, the value of flank wear and temperature was significantly high in comparison with the first two levels of feed and speed used. Decline in cutting force with increase in speed was due to thermal softening and hydrodynamic effect (as explained in Section 3.2). Further, it was indicated that by varying the feed from 0.05 to 0.10 rev/mm, not much difference in the value of flank wear, temperature, and cutting force was observed. On the basis of preliminary experiments, for main experimentation, final machining parameters (V_c, f, a_p) with four different environments as T1, T2, T3, and T4 are given in Table 9.

Table 7 Cutting conditions for preliminary experiments

Parameter	Unit	Level 1	Level 2	Level 3
V_c	m/min	80	130	200
f	mm/rev	0.05	0.10	0.15
a_p	mm	0.2	0.2	0.2
Graphene wt%	1.0 wt%			

Table 8 Output results of preliminary experiments

V_c (m/min)	f (mm/rev)	Flank wear (μm)	Temperature (°C)	Main cutting force, F_z (N)
80	0.05	45	415	212
130	0.10	58	580	203
200	0.15	135	610	190

3 Results and discussion

In this section, detailed experimental results are summarized. Performance of turning w.r.t. cutting forces, maximum flank wear (VB_{max}), cutting temperature, and graphene characterization are presented. In this work, under every machining environment, irregular wear marks on flank face were noticed as illustrated in Fig. 5. Hence, rather than VB, VB_{max} was preferred, because it was more authentic to compute under this state. Hence, $VB_{max} \leq 200$ μm specified in ISO-3685 was chosen and is compatible with precision hard-turning practices [36]. Thus experiments were stopped when the VB_{max} reached 200 μm. For measurement of tool wear, SEM/optical microscope was used, and cutting forces were obtained by digital microcontroller based lathe tool dynamometer coupled with computer through data acquisition system. Temperature generated throughout the cutting process was measured with an infrared optical probe. It has measurement range of − 50 to 900 °C with ± 0.75 °C accuracy. The entire temperature measuring system was previously calibrated as per ASTM E2847 standard. The mean values of the maximum temperature at nose of the tool, acquired in three times repeated experiments, were taken as final cutting temperatures. With the aid of confocal Raman spectroscopy, SEM, and optical microscope, various tool wear forms and lubrication tendency of graphene was examined.

3.1 Tool wear

Tool wear largely depends upon cooling/lubrication environment. Thus, to check the tribological behavior of graphene, it is important to quantify the tool flank wear. VB_{max} was measured in reference to cutting speed under various machining

Table 9 Final machining conditions

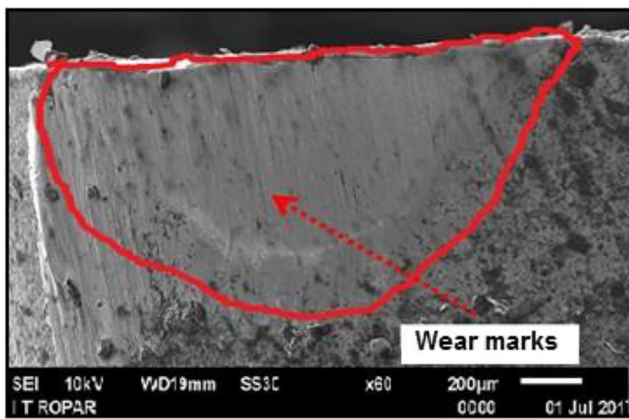| Parameters	Machining conditions
Cutting speed (V_c)	V_c = 80,130,180 m/min
Feed (f)	f = 0.10 mm/rev
Depth of cut (a_p)	a_p = 0.2 mm
MQL supply	Air = 6 bar, flow rate = 120 ml/h, nozzle distance from cutting edge = 30 mm, nozzle direction angle = 45° (with horizontal)
Graphene wt%	1.0

**Fig. 5** Flank face showing wear marks

conditions as depicted in Fig. 6(a). The results showed that the highest tool life as illustrated in Fig. 6(b) was achieved with T4 condition followed by T3 and T2 and finally under T1. As compared with dry condition (T1), tool life under NMQL (T4) was found to be increased by 178–190% at various cutting speeds. Figure 7(a, b) indicates the worn flank face and rake face of the cutting tool under T1 condition. Due to absence of any lubrication, the chip-curl diameter was considerably higher owing to larger tool-chip contact area which generated higher temperature at the tool cutting edge (supported by temperature graph in Section 3.3) led to adhered/welded chips to the rake face of the cutting tool, which further led to removing of this unwanted material from the tool surface and resulted in fracture of the tool edge [37]. Thus, the crater wear was high under this condition when no graphene was used, as shown in Fig. 7(b).

The lowest value of flank wear under T4 was mainly due to both lubrication and cooling action of graphene particles mixed in vegetable oil [16, 38, 39]. Further, it was observed that under T4, graphene participated both at rake face/cutting edge of the insert (Fig. 8) and performed shearing action of graphene layers. The presence of graphene particles resulted in lowest chip-curl diameter and led to reduced tool-chip contact area as well as crater wear on the rake face of cutting tool, as depicted in Fig. 8. Graphene without any difficulty moves

into the sliding contact surfaces and shears, due to its 2D configuration. This indicates the shear of covalently bonded one layer with respect to the other in graphene [39]. In addition, turning with NMQL (T4) resulted in faster removal of heat from the cutting zone due to higher thermal conductivity as well as wetting action of fluid mixture on the rake face of tool. [40]. The second best performance in tool life was achieved with T3 condition. In the case of T3, the dimples were full of graphene and acted as a lubricant between chip-tool interfaces by forming a dynamic lubricating film [41]. In order to identify the tribological response of graphene at the tool-chip contact surface, confocal Raman spectroscopy was employed to describe the feasibility of graphene to act as a lubricant between contact surfaces. Different authors [30, 42, 43] employed Raman spectroscopy to characterize the structure and morphology of ordered/disordered graphene, and they established that graphene developed a lubricating layer on sliding contact surfaces to enhance the tribological properties at the interface.

WITec Raman spectrometer with unpolarized Nd-YAG ion laser (532 nm) was used for characterization of graphene at rake face of cutting tool. The existence of graphene particles (ordered) within the dimple at point A is confirmed with Raman spectra of the 2D peak (~ 2700 cm^{-1}), i.e., the highest intensity and G-band peak at (1582 cm^{-1}) as shown in Fig. 9(a, c). Point A is a location on the rake face of the tool at which graphene has not yet worn out. Point B in Fig. 9(a, b) revealed that due to friction, majority of the graphene particles were distorted near the tool cutting edge. In this case, the 2D peak of graphene (at ~ 2700 cm^{-1}) was weak as compared with the ordered graphene, whereas one new peak, i.e., defect peak D (at ~ 1350 cm^{-1}), was generated, signifying that graphene was transformed to a disordered graphene due to alterations during sliding of chips on the rake surface of textured inserts [40, 43]. Distorted graphene indicated the participation of graphene to reduce the friction between tool-chip contact surface [42]. From this, it was clear that graphene dispersed in oil, apart from enhancing thermal conductivity, also offered enhanced lubrication with textured carbide tools during NMQL turning of Ti-6Al-4V.

Fig. 6 (a) Flank wear (VB$_{max}$) after 5 min of machining time. (b) Tool life up to 200 μm of flank wear at different cutting speed
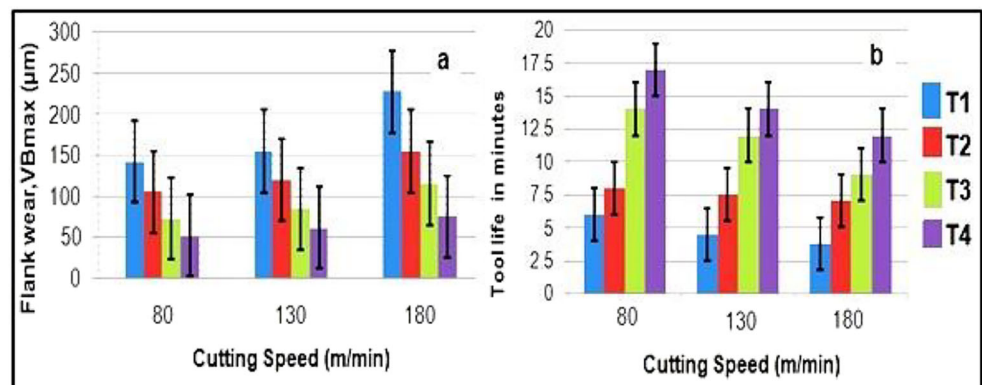
Fig. 7 (a) Worn flank face. (b) Crater wear after 5 min of machining with T1 condition at speed of 180 m/min
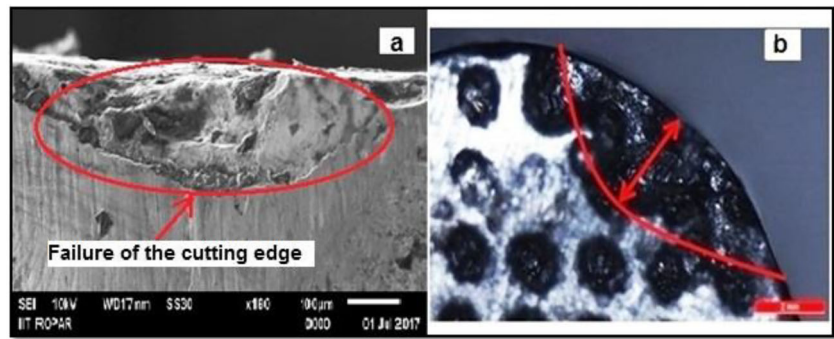

In T2, the flank wear was high as compared with T3 and T4 conditions. This was mainly due to an absence of graphene. Under this condition, canola oil evaporated more rapidly and therefore it was unable to keep a strong lubrication layer on the tool rake face [10]. This fact of evaporation of vegetable oil is also clear from the findings of cutting temperature as explained in Section 3.3. Ineffective lubrication/cooling under T2 led to high flank as well as crater wear on the cutting tool as presented in Fig. 10. Therefore, from the above discussion, it is clear that the best performance of T4 was mainly due to enhanced thermal conductivity and better tribological behavior of graphene mixed in vegetable oil under MQL [16, 40, 43]. This implies that NMQL lubrication is the sustainable means of reducing tool wear and improving the overall turning of Ti-6Al-4V.
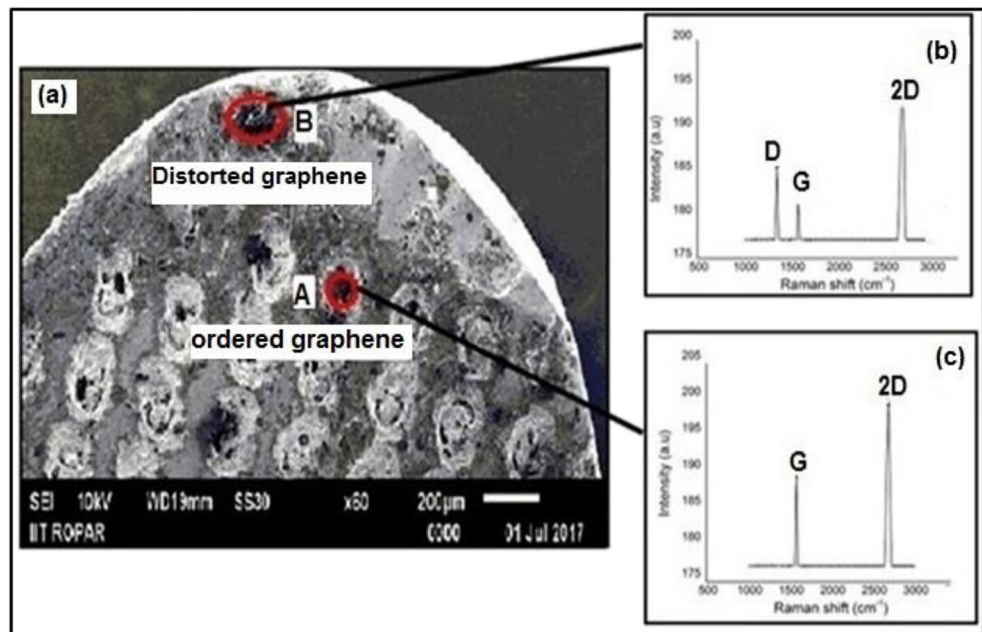
3.2 Cutting force

Cutting forces can provide a better understanding of lubrication and cooling effect during turning. Figure 11 illustrates the variations of cutting forces under the effect of various cooling /lubricating environments at varying cutting speed. The lowest cutting forces were obtained under T4 (NMQL) condition followed by T3, T2, and T1. Compared with the dry condition, cutting forces (i.e., F_x, F_y, and F_z) under T4 condition found to be reduced by 50–65%, 38–40%, 36–40% at varying cutting speeds. The cutting forces were decreased due to adequate hydrodynamic lift force provided by the fluid/solid lubricant in texture pockets (T2, T3, T4) as compared with dry state (T1) [44]. When speed increases, hydrodynamic lift force effect was more dominant and due to this trapped lubricant within the dimples comes out of the pockets under T2, T3, and T4 as compared with dry state and acted as a cooling/lubricating agent. Further under the dry environment, the performance of textured tool was very much similar to the previous reported works [45]. From Fig. 11, it was observed, irrespective of cooling/lubrication conditions, under all cutting speeds, all the three components of force reduced when graphene was used as a lubricant in comparison with other conditions. The reduction in cutting forces using graphene strengthens the fact that graphene showed best tribological behavior at tool-chip and tool-work material contact area

Fig. 8 SEM image of graphene particles: (a) Rake face. (b) Flank face of T4 and their corresponding EDX analysis
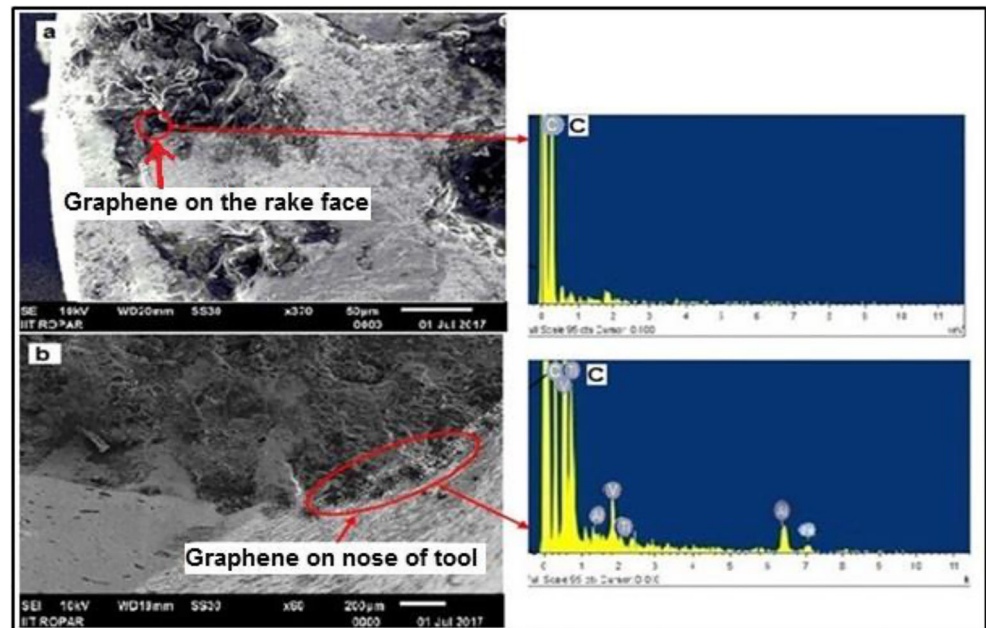
Fig. 9 (a) Rake face SEM image of T3 condition. (b) Raman spectra of disordered graphene at point B. (c) Raman spectra of ordered graphene at point A


due to its sharing behavior [16, 40]. Under every cutting environment with increase in cutting speed, the cutting forces decreases largely owing to the thermal softening of the work material [19, 22, 44]. It was observed that cutting forces significantly lowered under graphene environment, mostly at lowest and middle speed used as compared with maximum speed tested. It was due to enhanced lubricating results of graphene at low and middle cutting speed. This finding indicates that the effect of graphene to act as lubricant reduces with increase in speed. It was due to the fact that at highest cutting speed graphene was rapidly converted into the disordered graphitic structure [42]. T4 condition resulted in minimum forces as compared with all other conditions, due to the fact that used graphene nanoparticles penetrated and entrapped into the interface with mist droplets and thus led to thermal conduction and better lubrication under NMQL. Layered structure of graphene led to lowest friction, reduced cutting forces, and thus effective lubrication.
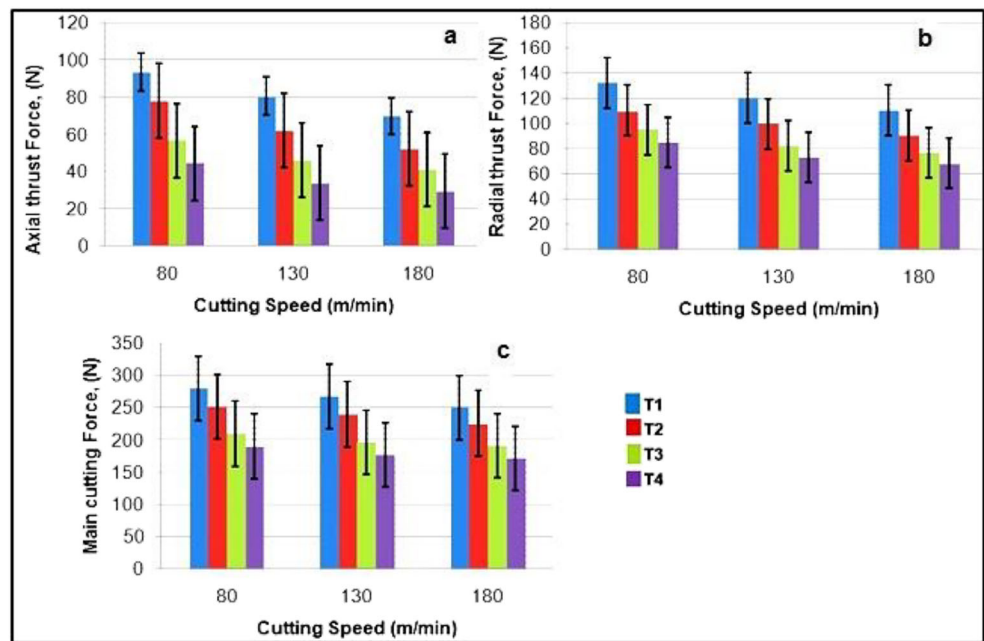
3.3 Cutting temperature

Figure 12 showed the mean cutting temperature near the cutting edge under four different environments at varying cutting speeds. The temperature values lies in between 330 and 701 °C. Cutting temperatures under T4, T3, and T2 were 31–42%, 17–28%, and 10–16% lower than the dry condition (T1) at different cutting speeds. The maximum cutting temperature was noticed under dry condition. It was primarily due to lack of any lubricating/cooling effect [3]. The lowest cutting temperature was observed under T4 condition in which nanoparticle mixed with oil was continuously sprayed on the cutting zone. The reduction in temperature was achieved under NMQL was mostly due to the improved thermal conductivity of NMQL and successful lubrication at tool-chip/tool-workpiece contact surface [16]. The value of cutting temperature achieved under T2 condition was significantly higher than T4, which was due to the fact that both heat carrying capacity and

Fig. 10 (a) Crater wear. (b) Flank wear after 5 min of machining with T2 condition at speed of 180 m/min
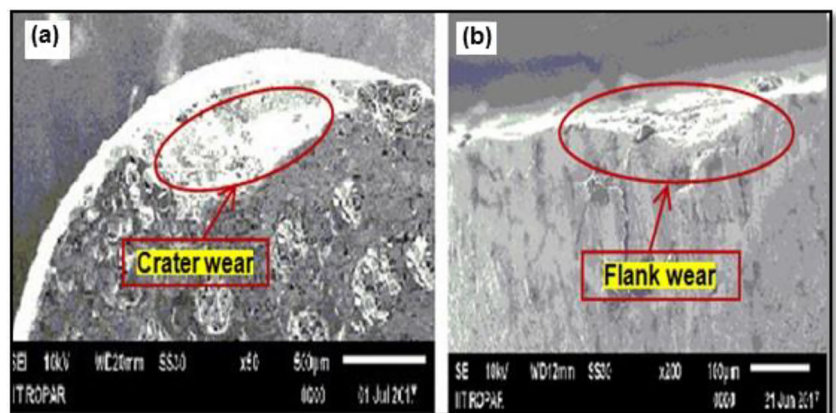
Fig. 11 Average value of cutting forces observed under different conditions: (a) axial thrust force– F_x; (b) radial thrust force— F_y; (c) main cutting force— F_z

the lubricating effect were low when only oil was used as compared with NMQL mixture [10]. Cutting temperature under T3 was 12% to 14% more than the T4 condition, which was mainly due to the absence of cooling effect under this condition and non-availability of continuous supply of fluid mixture. The temperature value was lower with T3 which was mainly due to effective lubrication offered by graphene at the tool-chip contact surface in comparison with only oil used under MQL (T2).

4 Conclusions

This work was aimed to evaluate the effect of graphene to be used as environmental friendly lubricant when mixed with canola oil in turning of Ti-6Al-4V. From the experimental investigations, the following conclusions were drawn.
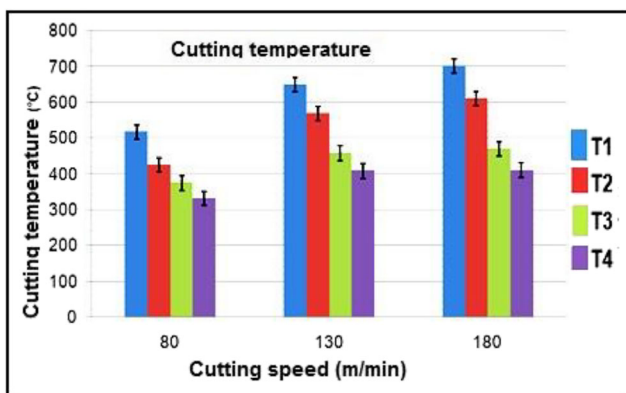
Fig. 12 Variation of average cutting temperatures with change in speed

1. Optimization of critical parameters for fabrication of textures on the rake face of cutting tool was carried out. Effective texture area was found to be (6.90 mm^2) for generation of texture patterns on the rake face. From preliminary experiments, the edge distance of 150 μm was found to be effective for imparting good edge strength to the cutting edge where no chipping on the cutting edge of tool was observed.

2. The results indicated that with the addition of graphene, the thermal conductivity of oil mixture in NMQL enhanced. On the basis of thermal conductivity test and suspension stability test, the optimized wt% of graphene loading was found to be "1" wt% out of 0.2, 0.5, and 2.0 wt% tested.

3. The order of turning performance under different environments was graphene-mixed vegetable oil (T4/NMQL) > texture filled with graphene particles (T3) > only vegetable oil (T2/MQL) > dry turning (T1). The best performance was achieved with NMQL, as under NMQL graphene-oil fluid mixture, was continuously available at the cutting tool. While under T3 condition, graphene availability reduces with the passage of time. Application of graphene mixed in canola oil under NMQL condition led to reduced friction between tool-chip as well as tool-workpiece contact surfaces. This also resulted in effective cooling of the cutting zone, due to enhanced thermal conductivity of fluid mixture. The use of only vegetable oil under MQL was not much effective as compared with NMQL (graphene-mixed solution). This was mainly due to low heat carrying capacity and poor lubrication effect of oil in comparison with graphene mixed in oil. But,

turning performance using vegetable oil under MQL was better than the dry condition.

4. As compared with dry condition (T1), tool life under NMQL was found to be increased by 178–190% at various cutting speeds. Lower tool wear/high tool life with NMQL was mainly owing to the shearing or deformation of graphene layers which led to effective lubrication/cooling action and low friction. In T3 condition, confocal Raman spectroscopy confirmed that distorted graphene particles near the cutting edge helped in lowering the friction between chip-tool contact surfaces thus, resulted in reduced tool wear. Under MQL, the use of only canola oil results in poor performance as compared with T2 and T3 conditions. But the performance was better than dry condition, as canola oil with rise in temperature evaporated faster and was unable to sustain the lubricating layer at tool rake face. Under dry environment at highest cutting speed (180 m/min), tool underwent catastrophic failure due to absence of any lubrication.

5. Under NMQL, both cutting forces and temperature generated were lowest as compared with all other environments. Further, it was observed that main cutting force (F_z) and cutting temperature with NMQL were 36–40% and 31–42% was lower than dry condition.

6. Finally, it was concluded that graphene has potential to act as lubricant/coolant in turning processes. But from the experiments it was revealed that at low and medium cutting speeds, the effectiveness of graphene was good. However, at highest cutting speed tested, fast conversion of disordered graphitization was observed by which graphene loses its effectiveness to act as lubricant.

7. In the future, the turning performance of multi-layer (between 5 and about 10 layers) graphene nanoparticles for cooling/lubrication along with wettability of textured cutting tool will be studied.

References

1. Mia M, Dhar NR (2018) Effects of duplex jets high-pressure coolant on machining temperature and machinability of Ti-6Al-4V superalloy. J Mater Process Technol 252:688–696. https://doi.org/10.1016/j.jmatprotec.2017.10.040
2. Maruda RW, Krolczyk GM, Wojciechowski S, Zak K, Habrat W, Nieslony P (2018) Effects of extreme pressure and anti-wear additives on surface topography and tool wear during MQCL turning of AISI 1045 steel. 32:1585–1591. https://doi.org/10.1007/s12206-018-0313-7
3. Krolczyk GM, Maruda RW, Krolczyk JB, Wojciechowski S, Mia M, Nieslony P, Budzik G (2019) Ecological trends in machining as a key factor in sustainable production–A review. JClean Prod 218:601–615
4. Gupta MK, Sood P (2017) Machining comparison of aerospace materials considering minimum quantity cutting fluid: a clean and green approach. Proc Inst Mech Eng C J Mech Eng Sci 231:1445–1464. https://doi.org/10.1177/0954406216684158
5. Dureja JS, Singh R, Singh T, Singh P, Dogra M, Bhatti MS (2015) Performance evaluation of coated carbide tool in machining of stainless steel (AISI 202) under minimum quantity lubrication (MQL). Int J Precis Eng Manuf Technol 2:123–129. https://doi.org/10.1007/s40684-015-0016-9
6. Sharma N, Gupta K (2019) Influence of coated and uncoated carbide tools on tool wear and surface quality during dry machining of stainless steel 304. Mater Res Express 6:086585. https://doi.org/10.1088/2053-1591/ab1e59
7. Sen B, Hussain SAI, Mia M, Mandal UK, Mondal SP (2019) Selection of an ideal MQL-assisted milling condition: an NSGA-II-coupled TOPSIS approach for improving machinability of inconel 690. Int J Adv Manuf Technol 103:1811–1829. https://doi.org/10.1007/s00170-019-03620-6
8. Singh T, Singh P, Dureja JS, Dogra M, Singh H, Bhatti MS (2016) A review of near dry machining/minimum quantity lubrication machining of difficult to machine alloys. Int J Mach Mach Mater 18:213–251. https://doi.org/10.1504/IJMMM.2016.076276
9. Dogra M, Sharma VS, Dureja JS, Gill SS (2018) Environment-friendly technological advancements to enhance the sustainability in surface grinding- a review. J Clean Prod 197:218–231. https://doi.org/10.1016/j.jclepro.2018.05.280
10. Oliveira D, Carvalho A, Rosa L, Jackson MJ, Machado ÁR (2019) Performance evaluation of vegetable-based cutting fluids in turning of AISI 1050 steel. Int J Adv Manuf Technol 103:1603–1619. https://doi.org/10.1007/s00170-019-03636-y
11. Dong L, Li C, Bai X, Zhai M, Qi Q, Yin Q, Lv X, Li L (2019) Analysis of the cooling performance of Ti – 6Al – 4V in minimum quantity lubricant milling with different nanoparticles. Int J Adv Manuf Technol 103:2197–2206
12. Pereira O, Alfonso JEM, Rodriguez A, Calleja A, Valdivielso AF, López de Lacalle LN (2017) Sustainability analysis of lubricant oils for minimum quantity lubrication based on their tribo-rheological performance. J Clean Prod 164:1419–1429. https://doi.org/10.1016/j.jclepro.2017.07.078
13. Rapeti P, Pasam VK, Gurram KMR, Revuru RS (2018) Performance evaluation of vegetable oil based nano cutting fluids in machining using grey relational analysis-a step towards sustainable manufacturing. J Clean Prod 172:2862–2875. https://doi.org/10.1016/j.jclepro.2017.11.127
14. Bai X, Li C, Dong L, Yin Q (2019) Experimental evaluation of the lubrication performances of different nanofluids for minimum quantity lubrication (MQL) in milling Ti-6Al-4V. Int J Adv Manuf Technol 101:2621–2632
15. Su Y, Gong L, Li B, Liu Z, Chen D (2016) Performance evaluation of nanofluid MQL with vegetable-based oil and ester oil as base fluids in turning. Int J Adv Manuf Technol 83:2083–2089. https://doi.org/10.1007/s00170-015-7730-x
16. Yi S, Li N, Solanki S, Mo J, Ding S (2019) Effects of graphene oxide nano fluids on cutting temperature and force in machining Ti-6Al-4V. Int J Adv Manuf Technol 103:1481–1495
17. Maruda RW, Krolczyk GM, Michalski M, Nieslony P, Wojciechowski S (2017) Structural and microhardness changes after turning of the AISI 1045 steel for minimum quantity cooling lubrication. J Mater Eng Perform 26:431–438. https://doi.org/10.1007/s11665-016-2450-4
18. Maruda RW, Feldshtein E, Legutko S, Krolczyk GM (2016) Analysis of contact phenomena and heat exchange in the cutting zone under minimum quantity cooling lubrication conditions. Arab J Sci Eng 41:661–668
19. Ranjan P, Hiremath SS (2019) Role of textured tool in improving machining performance: a review. J Manuf Process 43:47–73. https://doi.org/10.1016/j.jmapro.2019.04.011

20. Ge D, Deng J, Duan R, Liu Y, Li X, Yue H (2019) Effect of micro-textures on cutting fluid lubrication of cemented carbide tools. Int J Adv Manuf Technol 103:3887–3899

21. Sharma V, Pandey PM (2017) Geometrical design optimization of hybrid textured self-lubricating cutting inserts for turning 4340 hardened steel. Int J Adv Manuf Technol 89:1575–1589. https://doi.org/10.1007/s00170-016-9163-6

22. Orra K, Choudhury SK (2018) Tribological aspects of various geometrically shaped micro-textures on cutting insert to improve tool life in hard turning process. J Manuf Process 31:502–513. https://doi.org/10.1016/j.jmapro.2017.12.005

23. Chen Y, Wang J, Chen M (2019) Enhancing the machining performance by cutting tool surface modifications: a focused review. Mach Sci Technol 23:477–509. https://doi.org/10.1080/10910344.2019.1575412

24. Arulkirubakaran D, Senthilkumar V, Kumawat V (2016) Effect of micro-textured tools on machining of Ti-6Al-4V alloy: an experimental and numerical approach. Int J Refract Met Hard Mater 54:165–177. https://doi.org/10.1016/j.ijrmhm.2015.07.027

25. Li N, Chen Y, Kong D, Tan S (2017) Experimental investigation with respect to the performance of deep submillimeter-scaled textured tools in dry turning titanium alloy Ti-6al-4V. Applied Sur Sci. 403:187–199

26. Hao X, Li H, Yang Y, Xiao S, Song X, Li L (2019) Experiment on cutting performance of textured cemented carbide tools with various wettability levels. Int J Adv Manuf Techno 103:757–768

27. Kiyota H, Itoigawa F, Nakamura T (2014) Experimental research of micro-textured tool for reduction in cutting force. Key Eng Mater 611-612:1258–1263. https://doi.org/10.4028/www.scientific.net/KEM.611-612.1258

28. Obikawa T, Kamio A, Takaoka H, Osada A (2011) Micro-texture at the coated tool face for high performance cutting. Int J Mach Tools Manuf 51:966–972. https://doi.org/10.1016/j.ijmachtools.2011.08.013

29. Yu H, Deng H, Huang W, Wang X (2011) The effect of dimple shapes on friction of parallel surfaces. Proc Inst Mech Eng J J Eng Tribol 225:693–703. https://doi.org/10.1177/1350650111406045

30. Berman D, Erdemir A, Sumant AV (2014) Graphene: a new emerging lubricant. Mater Today 17:31–42. https://doi.org/10.1016/j.mattod.2013.12.003

31. Li P, Liu H, Chen H, Cheng X (2018) The influence of APTES interlayer on the assembly and tribological properties of graphene coatings on titanium substrate. Mater Res Express 6:16424. https://doi.org/10.1088/2053-1591/aae871

32. Xue B, Liu X, Shi X, Huang Y, Lu G, Wu C (2018) Effect of graphene nanoplatelets on tribological properties of titanium alloy matrix composites at varying sliding velocities. Mater Res Express 5:66507. https://doi.org/10.1088/2053-1591/aac703

33. Balandin AA, Ghosh S, Bao W, Calizo I, Teweldebrhan D, Miao F, Lao CN (2008) Superior thermal conductivity of single-layer graphene. Nano Lett 8:902–907. https://doi.org/10.1021/nl0731872

34. Lee GH, Cooper RC, An SJ, Lee S, Zhande A, Petrone N, Hammerberg AG, Lee C, Crawford B, Oliver W, Kysar JW, Hone J (2013) High-strength chemical-vapor deposited graphene and grain boundaries. Science 340:1073–1076. https://doi.org/10.1126/science.1235126

35. Ueda T, Hosokawa A, Yamada K (2005) Effect of oil mist on tool temperature in cutting. J Manuf Sci Eng 128:130–135

36. Dogra M, Sharma VS, Sachdeva A, Suri NM, Dureja JS (2011) Performance evaluation of CBN, coated carbide, cryogenically treated uncoated/coated carbide inserts in finish-turning of hardened steel. Int J Adv Manuf Technol 57:541–553. https://doi.org/10.1007/s00170-011-3320-8

37. Chinchanikar S, Choudhury SK (2014) Hard turning using HiPIMS-coated carbide tools: wear behavior under dry and minimum quantity lubrication (MQL). J Int Meas Confed 55:536–548

38. Chu B, Singh E, Koratkar N, Samuel J (2013) Graphene-enhanced environmentally-benign cutting fluids for high-performance micromachining applications. J Nanosci Nanotechnol 13:5500–5504

39. Singh RK, Sharma AK, Dixit AR, Tiwari AK, Pramanik A, Mandal A (2017) Performance evaluation of alumina-graphene hybrid nano-cutting fluid in hard turning. J Clean Prod 162:830–845

40. Sharma AK, Tiwari AK, Dixit AR, Singh RK, Singh M (2018) Novel uses of alumina/graphene hybrid nanoparticle additives for improved tribological properties of lubricant in turning operation. Tribol Int 119:99–111. https://doi.org/10.1016/j.triboint.2017.10.036

41. Jianxin D, Wenlong S, Hui Z (2009) Design, fabrication and properties of a self-lubricated tool in dry cutting. Int J Mach Tools Manuf 49:66–72. https://doi.org/10.1016/j.ijmachtools.2008.08.001

42. Wu L, Gu L, Xie Z, Zhang C, Song B (2017) Improved tribological properties of Si3N4/GCr15 sliding pairs with few layer graphene as oil additives. Ceram Int 43:14218–14224. https://doi.org/10.1016/j.ceramint.2017.07.168

43. Kaniyoor A, Ramaprabhu S (2016) A Raman spectroscopic investigation of graphite oxide derived graphene A Raman spectroscopic investigation of graphite oxide derived graphene. AIP Adv 2:032183. https://doi.org/10.1063/1.4756995

44. Stoeterau RL, Janssen A, Mallmann G (2017) Analysis of dimple textured surfaces on cutting tools. J Braz Soc Mech Sci Eng 39:3989–3996. https://doi.org/10.1007/s40430-016-0692-6

45. Ze W, Jianxin D, Yang C, Youqiang X, Jun Z (2012) Performance of the self-lubricating textured tools in dry cutting of Ti-6Al-4 V. Int J Adv Manuf Technol 62:943–951. https://doi.org/10.1007/s00170-011-3853-x